

# Coexistence of two electronic phases in $\text{LaTiO}_{3+\delta}$ ( $0.01 \leq \delta \leq 0.12$ ) and their evolution with $\delta$

H. D. Zhou and J. B. Goodenough

Texas Materials Institute, ETC 9.102, The University of Texas at Austin, 1 University Station, C2201, Austin, Texas 78712, USA

(Received 16 November 2004; published 29 April 2005)

Although  $\text{LaTiO}_{3+\delta}$  ( $0.01 \leq \delta \leq 0.12$ ) is single-phase to powder x-ray diffraction, its properties reveal that a hole-poor strongly correlated electronic phase coexists with a hole-rich itinerant-electron phase. With  $\delta \leq 0.03$ , the hole-rich phase exists as a minority phase of isolated, mobile itinerant-electron clusters embedded in the hole-poor phase. With  $\delta \geq 0.08$ , isolated hole-poor clusters are embedded in an itinerant-electron matrix. As  $\delta > 0.08$  increases, the hole-poor clusters become smaller and more isolated until they are reduced to superparamagnetic strong-correlation fluctuations by  $\delta = 0.12$ . This behavior is consistent with prediction from the virial theorem of a first-order phase change at the crossover from localized (or strongly correlated) to itinerant electronic behavior, a smaller equilibrium (Ti-O) bond length being in the itinerant-electron phase. Accordingly, the variation of volume with oxidation state does not obey Végard's law; the itinerant-electron minority phase exerts a compressive force on the hole-poor matrix, and the hole-poor minority phase exerts a tensile stress on the hole-rich matrix.

DOI: 10.1103/PhysRevB.71.165119

PACS number(s): 71.30.+h, 72.20.Pa, 72.80.Ga, 75.30.Cr

## I. INTRODUCTION

$\text{LaTiO}_3$  is an orthorhombic ( $c/a > \sqrt{2}$  in space group  $Pbnm$ ) perovskite with a single  $\pi$ -bonding  $3d$  electron per octahedral-site Ti(III). The Coulomb repulsion between electrons splits the occupied Ti(IV)/Ti(III) and empty Ti(III)/Ti(II) redox couples by a small, but finite energy gap  $E_g \approx 0.2$  eV.<sup>1</sup> A rhombohedral distortion of the  $\text{TiO}_{6/2}$  octahedra appears to stabilize  $3d$ -electron density along a [111] axis, which can account for antiferromagnetic Ti-O-Ti interactions between all nearest neighbors;<sup>2</sup>  $\text{LaTiO}_3$  is an antiferromagnetic insulator with a weak canted-spin ferromagnetic component below a Néel temperature  $T_N \approx 140$  K (Refs. 1,3) and a titanium magnetic moment of only  $0.46 \mu_B$  as determined by neutron diffraction.<sup>4</sup> However, whether  $\text{LaTiO}_3$  is an itinerant- or a localized-electron antiferromagnet remains controversial.

The system  $\text{La}_{1-x}\text{Sr}_x\text{TiO}_3$  exhibits broadband metallic behavior for  $x > 0.5$ , but as  $x < 0.5$  decreases, an increasing enhancement of the electron effective mass  $m^*$  as a result of increasing electron-electron Coulomb interactions.<sup>5-7</sup> A first-order metal-insulator transition occurs in the interval  $0.04 \leq x \leq 0.08$ .<sup>8</sup> Substitution of the larger  $\text{Sr}^{2+}$  ion for  $\text{La}^{3+}$  not only introduces holes into the Ti(IV)/Ti(III) couple, it also straightens the  $(180^\circ - \phi)$  Ti-O-Ti bonds, which broadens the narrow  $\pi^*$  bands, without perturbing too strongly the periodic potential experienced by the Ti- $3d$  electrons.

An alternative way to introduce an insulator to metal transition in  $\text{LaTiO}_3$  is to increase its oxidation state.<sup>9</sup> Although it is customary to express the oxidized compounds as  $\text{LaTiO}_{3+\delta}$ , the perovskite structure does not support the introduction of interstitial oxide ions; rather, the excess oxygen is accommodated by the introduction of cation vacancies. Since the  $\text{La}^{3+}$  ions are more mobile than the  $\text{Ti}^{4+}$  ions, the resulting  $\text{La}_{1-x}\text{Ti}_{1-y}\text{O}_3$  compositions have  $x > y$ .<sup>10</sup> The cation vacancies introduce a stronger perturbation of the periodic potential experienced by the Ti- $3d$  electrons than does substitutional  $\text{Sr}^{2+}$  ions. We report here a study that shows an

evolution with increasing  $\delta$  from hole-rich itinerant-electron clusters in a hole-poor insulating matrix to strongly correlated electron fluctuations in an itinerant-electron matrix across the interval  $0 < \delta \leq 0.12$ .

## II. EXPERIMENT

Polycrystalline samples of  $\text{LaTiO}_{3+\delta}$  ( $0.01 \leq \delta \leq 0.12$ ) and  $\text{LaTi}_{1-x}\text{Cr}_x\text{O}_3$  ( $x = 0.1$  and  $0.2$ ) were prepared by standard solid-state reaction. Stoichiometric mixtures of  $\text{La}_2\text{O}_3$ ,  $\text{Cr}_2\text{O}_3$ , and/or  $\text{Ti}_2\text{O}_3$  were ground together and cold-pressed into pellets; the pellets were placed into a molybdenum crucible put inside an evacuated tube ( $\sim 10^{-6}$  Torr) and fired for 12 h at temperatures varying from  $1350^\circ\text{C}$  to  $1620^\circ\text{C}$  to obtain different values of  $\delta$ . A Perkin-Elmer TGA-7 thermogravimetric analyzer (TGA) was used to determine the oxygen content of the  $\text{LaTiO}_{3+\delta}$  samples from the weight gain on oxidation of the Ti(III) ions to Ti(IV) on heating to  $1000^\circ\text{C}$  in air. Samples with  $\delta = 0.01, 0.015, 0.03, 0.05, 0.08, 0.10,$  and  $0.12$  (all with  $\pm 0.01$ ) were obtained after firing in vacuum at  $1620^\circ\text{C}, 1600^\circ\text{C}, 1550^\circ\text{C}, 1500^\circ\text{C}, 1450^\circ\text{C}, 1400^\circ\text{C},$  and  $1350^\circ\text{C}$ , respectively. The  $\text{LaTi}_{1-x}\text{Cr}_x\text{O}_3$  samples were fired in vacuum at  $1620^\circ\text{C}$ .

Powder x-ray diffraction (XRD) patterns were recorded with a Philips PW 1729 powder x-ray diffractometer equipped with a pyrolytic graphite monochromator and Cu  $K_\alpha$  radiation ( $1.54059 \text{ \AA}$ ); Si was the internal standard. Data were collected in steps of  $0.020^\circ$  over the range  $20^\circ \leq 2\theta \leq 60^\circ$  with a count time of 20 s per step. Peak profiles for the XRD data were fitted with the program JADE. All samples were single-phase to XRD.

Magnetic-susceptibility was measured with a Quantum Design dc SQUID magnetometer after cooling in either zero field (ZFC) or in a measuring field (FC) of 1 kOe. Hysteresis loops of magnetization  $M$  versus applied field  $H$  were obtained over the range  $-5 \text{ T} \leq H \leq 5 \text{ T}$  at 5 K.

The thermoelectric power  $\alpha(T)$  was measured from 80 K to 300 K with a laboratory-built apparatus as described

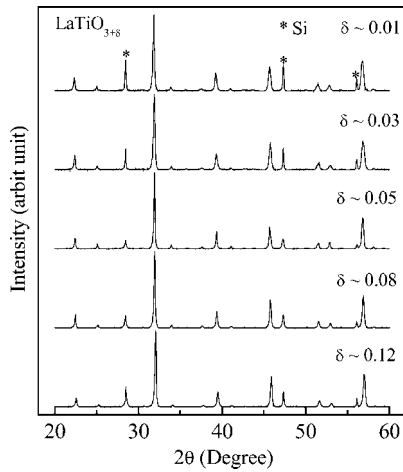


FIG. 1. XRD spectra for  $\text{LaTiO}_{3+\delta}$  samples.

elsewhere.<sup>11</sup> The resistivity was measured with a four-probe technique on samples that were cold-pressed as mixed powders. The cold-pressing technique has been described elsewhere.<sup>12</sup> The  $\rho(T)$  data obtained with our cold-pressed polycrystalline samples were similar to the single-crystal data reported by Okada *et al.*<sup>13</sup> and Katsufuji *et al.*<sup>14</sup>

III. RESULTS

All samples were single-phase, orthorhombic ( $Pbnm$  space group) perovskites to XRD, Fig. 1. Figure 2 shows the variation with  $\delta$  of the measured unit-cell volumes of  $\text{LaTiO}_{3+\delta}$ ,  $0.01 \leq \delta \leq 0.12$ . The volume decreases with increasing oxidation parameter  $\delta$ , but there is a dramatic change of the slope  $dV/d\delta$  near  $\delta=0.05$ .

Figure 3 shows that the resistivity of the  $\text{LaTi}_{1-x}\text{Cr}_x\text{O}_3$  samples remain semiconductive with an activated charge-carrier mobility, the motional enthalpy increasing from  $E_a = 0.035$  eV in  $\text{LaTiO}_{3.01}$  to  $E_a = 0.11$  eV for nominal  $\text{LaTi}_{0.8}\text{Cr}_{0.2}\text{O}_3$ . As  $\delta$  of  $\text{LaTiO}_{3+\delta}$  increases,  $\rho(T)$  evolves progressively above 50 K from (1)  $\rho(T) \sim \exp(-E_a/kT)$  for  $\delta=0.01$  to (2) a  $\rho(T) \sim \exp(T_0/T)^{1/4}$ , which is characteristic of variable-range hopping, in the range  $150 \text{ K} \leq T \leq 300 \text{ K}$

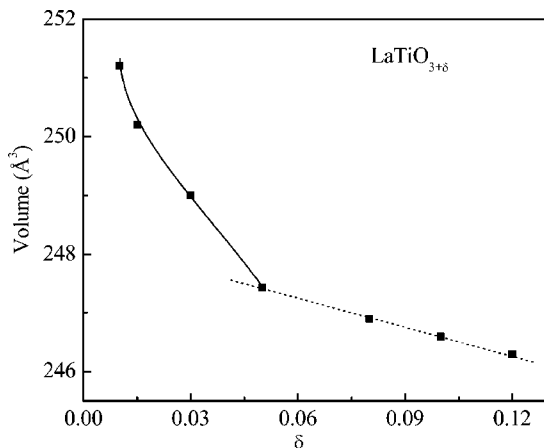


FIG. 2. Variation with  $\delta$  of unit-cell volume for  $\text{LaTiO}_{3+\delta}$ .

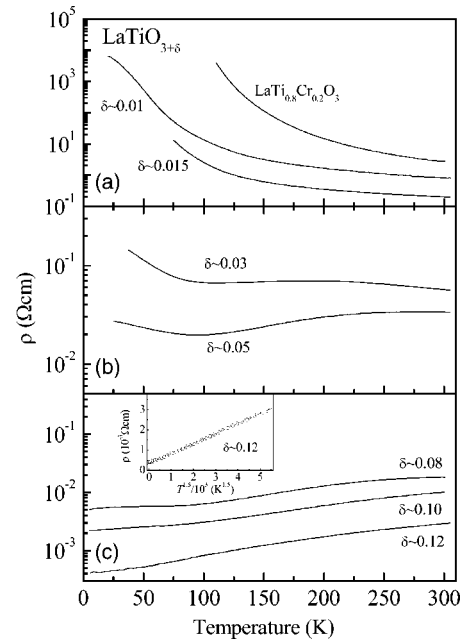


FIG. 3. Temperature dependencies of resistivity  $\rho$  for samples of  $\text{LaTiO}_{3+\delta}$  and  $\text{LaTi}_{0.8}\text{Cr}_{0.2}\text{O}_3$ . Inset of (c):  $T^{-1.5}$  dependence of resistivity for  $\text{LaTiO}_{3.12}$ .

for  $\delta=0.015$  and  $200 \text{ K} \leq T \leq 300 \text{ K}$  for  $\delta=0.03$ , followed by (3) a smooth semiconductor to metal transition near 100 K for  $\delta=0.05$  before exhibiting (4) a metallic temperature dependence over the entire temperature range from 40 K to 300 K for  $\delta \geq 0.08$ , but (5) with a  $\rho(T) = \rho_0 + aT^{3/2}$  over the range  $40 \text{ K} \leq T \leq 320 \text{ K}$  showing non-Fermi-liquid behavior remaining in the  $\delta=0.12$  sample.

The thermoelectric-power data  $\alpha(T)$  of Fig. 4 shows an evolution from  $p$ -type for  $\delta \leq 0.03$  to  $n$ -type conduction for

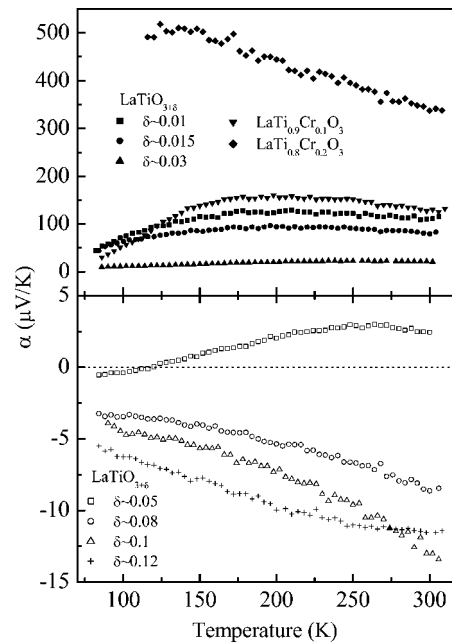


FIG. 4. Temperature dependencies of thermoelectric power  $\alpha$  for samples of  $\text{LaTiO}_{3+\delta}$  and  $\text{LaTi}_{1-x}\text{Cr}_x\text{O}_3$ .

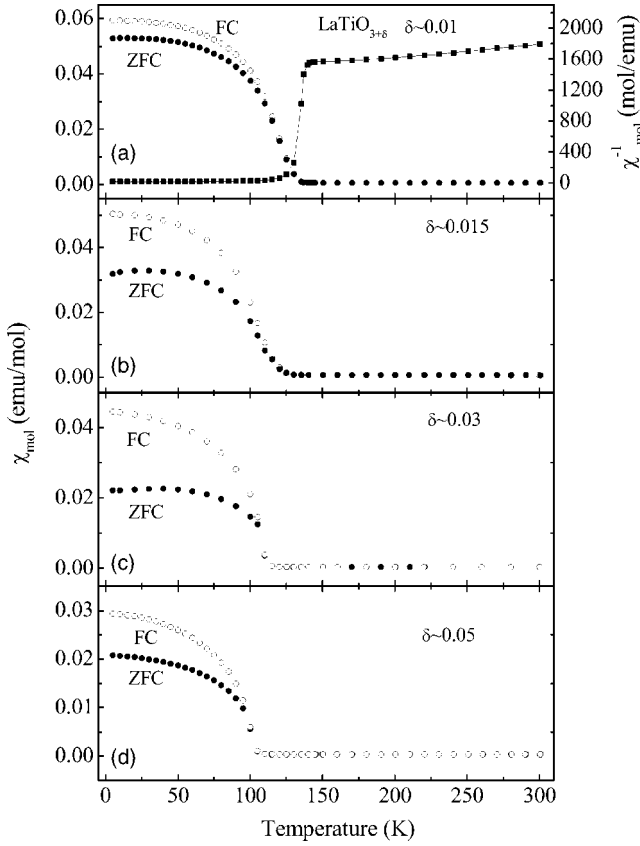


FIG. 5. (a) Molar magnetic susceptibility  $\chi_{\text{mol}}$  and its inverse  $1/\chi_{\text{mol}}$  of sample  $\text{LaTiO}_{3.01}$ ; (b, c, and d): Molar magnetic susceptibility  $\chi_{\text{mol}}$  for  $\text{LaTiO}_{3.015}$ ,  $\text{LaTiO}_{3.03}$ , and  $\text{LaTiO}_{3.05}$ , respectively.

$\delta \geq 0.08$  with an  $n$  to  $p$  crossover in the  $\delta=0.05$  sample where the room-temperature volume versus  $\delta$  curve, Fig. 2, shows a dramatic change of slope. Above 150 K,  $\alpha(T)$  for  $\text{LaTiO}_{3+\delta}$  ( $0.01 \leq \delta \leq 0.03$ ) is temperature-independent, which is characteristic of polaronic conduction. The magnitude of  $\alpha(T) > 0$  decreases with increasing  $\delta$  as expected for an increasing population of charge carriers. At room temperature, the  $\text{LaTiO}_{3.01}$  and nominal  $\text{LaTi}_{0.9}\text{Cr}_{0.1}\text{O}_3$  samples have a comparable  $\alpha(300 \text{ K}) \approx 120 \mu\text{V/K}$ ; but a weak temperature dependence of  $\alpha(T)$  for  $\text{LaTi}_{0.9}\text{Cr}_{0.1}\text{O}_3$  implies some trapping out of charge carriers at lower temperatures. The nominal  $\text{LaTi}_{0.8}\text{Cr}_{0.2}\text{O}_3$  sample shows a stronger trapping out of charge carriers below 300 K with a trapping enthalpy  $\Delta H_t/2 \approx 0.017 \text{ eV}$ . It is also noteworthy that  $\alpha(T) < 0$  for  $\delta = 0.12$  becomes temperature-independent above 250 K.

Figures 5–7 show, respectively, the magnetic susceptibilities of  $\text{LaTiO}_{3+\delta}$  for  $0.01 \leq \delta \leq 0.05$ ,  $\delta = 0.08$  and  $0.10$ ,  $\delta = 0.12$ . The appearance of a weak canted-spin ferromagnetism below a  $T_N = 140 \text{ K}$  in  $\text{LaTiO}_{3.01}$  is similar to that reported by other groups.<sup>1,3</sup> However, the inverse susceptibility,  $1/\chi_{\text{mol}}(T)$ , for the ZFC curve of  $\text{LaTiO}_{3.01}$ , Fig. 5(a), exhibits only a weak temperature dependence above  $T_N$  that is more characteristic of a strongly enhanced Pauli paramagnetism than of a localized-electron Curie-Weiss law even though strong electron correlations split the Ti(IV)/Ti(III) and Ti(III)/Ti(II) redox couples. Fitting the curve to a Curie-Weiss law gives a Weiss constant  $\theta \approx -1000 \text{ K}$ .

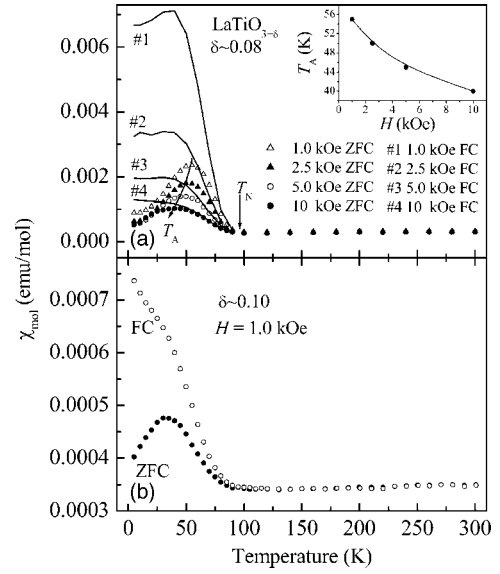


FIG. 6. Molar magnetic susceptibility  $\chi_{\text{mol}}$  for (a)  $\text{LaTiO}_{3.08}$  and (b)  $\text{LaTiO}_{3.10}$ . Inset of (a) Magnetic field dependence of  $T_A$  for ZFC curves of  $\text{LaTiO}_{3.08}$ .

Whereas the FC and ZFC  $M(T)/H$  curves of Fig. 5 all show normal ferromagnetic behavior with a progressive decrease with increasing  $\delta$  in the FC value of  $M/H$  at  $T = 5 \text{ K}$ , the ZFC  $M(T)/H$  curves for  $\delta = 0.08$  and  $0.10$  in Fig. 6 exhibit a small remanance at  $T = 5 \text{ K}$  with a maximum value of  $M/H$  at a  $T_A < T_N$ . Moreover, the FC values of  $M/H$  at  $T = 5 \text{ K}$  decrease more sharply with increasing  $\delta$  for  $\delta = 0.08$  and  $0.10$ . For  $\delta = 0.08$ ,  $T_A$  moves to lower temperature with increasing applied field in the range  $1 \text{ kOe} \leq H \leq 10 \text{ kOe}$ , inset of Fig. 6(a). In  $H = 1 \text{ kOe}$ , the FC value of  $M/H$  also shows a maximum, but this maximum progressively disappears with increasing the field to  $H = 10 \text{ kOe}$ . The  $\delta = 0.10$  sample has a maximum ZFC value of  $M(T)/H$  at a lower  $T_A = 32 \text{ K}$  and no maximum in the FC value of  $M(T)/H$ . Both the  $\delta = 0.08$  and the  $\delta = 0.10$  sample exhibit  $M-H$  hysteresis loops at  $5 \text{ K}$ , Fig. 8, that fail to saturate at  $5 \text{ T}$ . The  $\delta = 0.12$  sample shows no evidence of a long-range magnetic

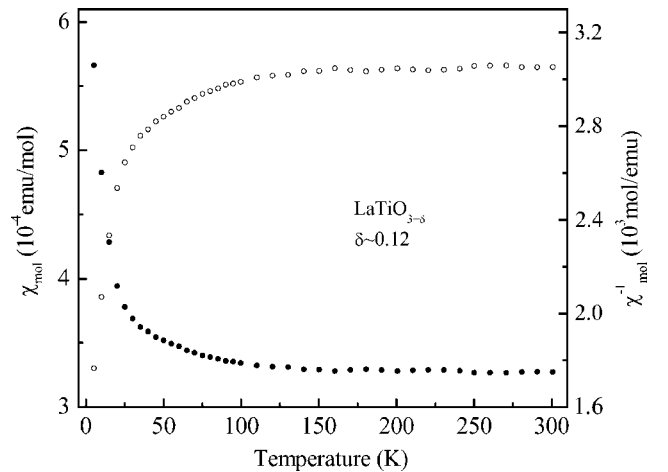


FIG. 7. Molar magnetic susceptibility  $\chi_{\text{mol}}$  and its inverse  $1/\chi_{\text{mol}}$  of sample  $\text{LaTiO}_{3.12}$ .

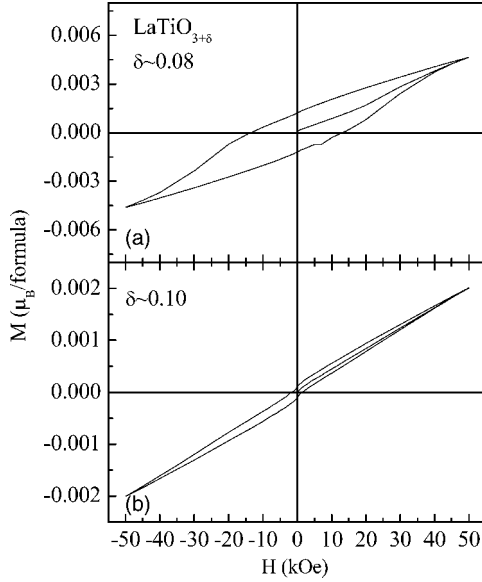


FIG. 8. Field dependence of magnetization measured at 5 K for (a)  $\text{LaTiO}_{3.08}$  and (b)  $\text{LaTiO}_{3.10}$ .

order, Fig. 7. Above 100 K, the susceptibility of Fig. 7 is essentially temperature-independent, but its magnitude is two orders of magnitude larger than that of the Pauli paramagnetism of a conventional metal; also, the susceptibility increases sharply with decreasing temperature below 100 K typical of the presence of localized-electron impurities.

#### IV. DISCUSSION

##### A. Samples with $\delta \approx 0.01$

Interpretation of the data for  $\text{LaTiO}_{3+\delta}$  depends on the model we choose for the development of cation vacancies with increasing  $\delta$ . For  $\delta=0.01$ , we assume that there are no vacancies on the  $\text{TiO}_3$  array, which would give  $x=0.0067$  in  $\text{La}_{1-x}\text{TiO}_3$  for 0.02 holes in the Ti(IV)/Ti(III) redox couple. If the temperature-independent  $\alpha(T) \approx 120 \mu\text{V}/\text{K}$  above 150 K signals polaronic behavior for all the holes, then the statistical contribution  $\alpha_s$  to  $\alpha(T)$  is dominant and would be given by<sup>15</sup>

$$\alpha_s = (k/e) \ln[\beta(1 - Qc)/Qc], \quad (1)$$

where  $k$  is the Boltzmann constant,  $e$  is the charge of the polaron,  $\beta=2$  is the spin-degeneracy factor,  $c$  is the fraction of Ti atoms that have the formal valence Ti(IV) in a small-polaron situation, and  $Q$  is the polaron size. A  $c=2\delta=0.02-0.04$  gives a  $Q=16-8$ , which corresponds either to a large polaron size or to the existence of itinerant-electron clusters in a matrix of strongly correlated electrons.

Three considerations favor the existence of itinerant-electron clusters. (1) From the Virial Theorem, it has been argued<sup>16</sup> that the transition from localized to itinerant electronic behavior is first-order and that where the resulting spinodal phase segregation occurs at too low a temperature for atomic diffusion, phase segregation in perovskite-related structures can be accommodated by locally cooperative

atomic displacements that, in a mixed-valent situation, may define a hole rich mobile cluster with low motional enthalpy embedded in an insulator matrix as is illustrated, for example, by the superconductive  $\text{La}_{2-x}\text{Sr}_x\text{CuO}_4$  system, the manganites  $\text{La}_{1-x}\text{Ca}_x\text{MnO}_3$  exhibiting the colossal magnetoresistance (CMR) phenomenon, and the  $\text{La}_{1-x}\text{Sr}_x\text{CoO}_3$  system.<sup>17</sup> (2) Fujimori *et al.*<sup>18</sup> have shown with photoemission spectroscopy (PES) the coexistence of electrons in Fermi-liquid states and in a lower Hubbard band in a  $\text{LaTiO}_{3+\delta}$  sample with  $\delta=0.03 \pm 0.01$ . (3) The system  $\text{La}_{1-x}\text{Sr}_x\text{TiO}_3$  approaches the Mott-Hubbard transition from the localized-electron side as  $x$  increases to  $x=0.05$ .<sup>5-7</sup>

Isolated, yet mobile, hole-rich itinerant-electron clusters in a matrix of strongly correlated electrons at Ti(III) ions would avoid coalescence by the Coulomb repulsion between them. Nevertheless, the fact that the mobile charge is distributed over several Ti centers reduces the locally cooperative oxide-ion displacements that self-trap the holes to clusters, which ensures a low motional enthalpy  $\Delta H_m$ .<sup>19</sup> The measured  $E_a = \Delta H_m = 0.035 \text{ eV}$  is over a factor 3 smaller than found with conventional small polarons. The  $\text{La}^{3+}$ -ion vacancies would trap strongly small-polaron holes, but mobile hole-rich clusters would be trapped much less strongly. A weak trapping energy is manifested below 50 K. The itinerant-electron clusters dilute the spin-spin exchange interactions between Ti(III) ions, which lowers  $T_N$ . The clusters would also introduce a Pauli paramagnetic component to the paramagnetic susceptibility, but a theory of how the susceptibility is made more temperature-independent by fluctuations between localized and itinerant electronic behavior at the Ti atoms is lacking. However, so long as the hole-poor matrix percolates, long-range antiferromagnetic order is stabilized.

The  $\text{Cr}^{3+}$ -ions in  $\text{LaTi}_{1-x}\text{Cr}_x\text{O}_3$  samples perturb the potential experienced by the Ti-3d electrons more strongly than do the  $\text{La}^{3+}$ -ion vacancies and would therefore tend to act as deeper traps for any hole-rich clusters. Nevertheless, the transport properties of nominal  $\text{LaTi}_{0.9}\text{Cr}_{0.1}\text{O}_3$  are similar to those of  $\text{LaTiO}_{3.01}$ ; it is only for larger  $\text{Cr}^{3+}$ -ion concentrations, as in  $\text{LaTi}_{0.8}\text{Cr}_{0.2}\text{O}_3$  where an itinerant-electron cluster encounters multiple  $\text{Cr}^{3+}$ -ions centers, that a stronger trapping out of holes becomes evident.

##### B. The $\delta=0.12$ sample

The other end sample,  $\text{LaTiO}_{3.12}$ , would have both La and Ti vacancies:  $\text{La}_{1-x}\text{Ti}_{1-y}\text{O}_3$  with  $x > y$ . The Ti vacancies would perturb the Ti-3d electronic potential of the  $\text{Ti}_{1-y}\text{O}_3$  array strongly enough to introduce Anderson localized states at the bottom of an itinerant-electron  $\pi^*$  band less than  $1/6$ -occupied. A Fermi energy  $\varepsilon_F$  a little above the mobility edge  $\mu_c$  would result in  $n$ -type metallic conduction. The observed  $\rho(T) = \rho_0 + aT^{3/2}$  behavior is incompatible with a Fermi liquid for electrons with  $\varepsilon > \varepsilon_F$ , but it has been predicted<sup>20</sup> for a narrow band containing strong-correlation fluctuations (SCFs) with an  $\varepsilon_F$  a little above a mobility edge. The general expression for the thermoelectric power is<sup>21</sup>

$$\alpha = -\frac{k}{e} \int \frac{(\varepsilon - \varepsilon_F) \sigma(\varepsilon)}{kT \sigma} d\varepsilon \quad (2)$$

in which  $\sigma(\varepsilon) = f(\varepsilon)[1 - f(\varepsilon)]N(\varepsilon)\mu(\varepsilon)$  is the product of the Fermi distribution functions  $f(\varepsilon)$  and  $[1 - f(\varepsilon)]$  for electrons

and holes, the energy density of one-electron states  $N(\varepsilon)$ , and the electron mobility  $\mu(\varepsilon)$  for energies  $\varepsilon$  taken from the bottom of the conduction band;  $\sigma$  is the electronic conductivity. A large difference between  $(\varepsilon - \varepsilon_F)\sigma(\varepsilon)$  for  $\varepsilon > \varepsilon_F$  and  $\varepsilon < \varepsilon_F$  for  $\varepsilon_F$  a little above  $\mu_c$  can give the large increase of  $\alpha(T)$  with temperature that is observed in the  $n$ -type samples  $0.08 \leq \delta \leq 0.12$ , and saturation above 250 K in  $\text{LaTiO}_{3.12}$  may signal the onset of vibronic states near  $\varepsilon_F$  at higher temperatures.

### C. $0.01 < \delta < 0.12$

The evolution of physical properties from those of  $\text{LaTiO}_{3.01}$  to those of  $\text{LaTiO}_{3.12}$  is smooth. The transition from hole-rich itinerant-electron clusters in a hole-poor matrix of strongly correlated electrons to strong-correlation fluctuations in an itinerant-electron matrix containing Anderson-localized states occurs near  $\delta=0.05$  where both volume fractions percolate at low temperatures. Although Fig. 4 shows that the  $\delta=0.03$  sample remains a  $p$ -type conductor, which indicates polaronic charge carriers in a matrix where the Ti(IV)/Ti(III) and Ti(III)/Ti(II) redox couples are split by strong electron-electron Coulomb interactions, the resistivity data of Fig. 3 shows a vanishing of the motional enthalpy of the charge carriers below 150 K with an up-turn below 100 K due to a trapping of the carriers. This indication that the volume fraction of the itinerant-electron regions grows with decreasing temperature is reinforced by the data of Fig. 4 for  $\delta=0.05$ , which show a crossover from  $p$ -type polaronic behavior at higher temperatures to  $n$ -type bad-metal behavior at lower temperatures. At this crossover composition,  $\delta=0.05$ , the itinerant-electron clusters apparently grow to beyond percolation with decreasing temperature, but Fig. 5 shows that the strongly correlated volume fraction also percolates to retain long-range magnetic order in the ZFC regime. However, the ZFC curves of Fig. 6 are characteristic of a cluster glass.<sup>22</sup> The transport properties of the samples  $\delta=0.08$  and  $0.10$  are dominated by the percolating itinerant-electron matrix, but the samples retain a significant volume of regions with strongly correlated electrons within which there is long-range magnetic order; these regions become smaller and more isolated from one another as  $\delta$  increases. Cooling in zero applied field (ZFC) leaves the isolated regions randomly oriented; they are only reoriented by the measuring field  $H$  as the temperature approaches  $T_N$  where the magnetocrystalline anisotropy is strongly reduced. Cooling in an applied field orients the separated regions, but weak coupling between regions allows local anisotropy fields to cause the regions to relax to differently oriented easy axes at lower temperatures unless the applied field is stronger than the effective anisotropy field. As  $\delta$  increases to  $\delta=0.12$ , the magnetic regions are reduced to strong-correlation fluctua-

tions that act like superparamagnetic impurities.

Given this smooth evolution of physical properties, it is of interest to return to Fig. 2. From the virial theorem, it was argued<sup>16</sup> that the equilibrium (Ti-O) bond length for strongly correlated electrons should be longer than that for itinerant electrons; it is the double-well character of the (Ti-O) bond potential at crossover that stabilizes separation into regions of hole-rich itinerant electrons and hole-poor strongly correlated electrons. Figure 2 shows that where the volume fraction of strongly correlated electrons is dominant, the volume decreases more sharply with increasing  $\delta$  than it does where the volume fraction of itinerant electrons is dominant. With a double-well bond potential, the larger equilibrium (Ti-O) bond is more compressible. The itinerant-electron regions impose a compressive stress on the hole-poor matrix whereas the hole-poor minority regions impose a tensile stress on the itinerant-electron matrix. Therefore, the sharp change in the slope of volume versus  $\delta$  in Fig. 2 occurs near  $\delta \approx 0.05$  where the matrix changes from the hole-poor to the hole-rich electronic phase. This argument is supported by transformation of the magnetic-insulator phase to the metallic phase by the application of hydrostatic pressure.<sup>13</sup>

## V. CONCLUSION

Examination of the evolution with oxidation state of the physical properties of  $\text{LaTiO}_{3+\delta}$  reveals that the Ti-3d electrons do not behave as localized electrons even in the lowest oxidation state,  $\delta=0.01 \pm 0.01$ , where the compound is an antiferromagnetic insulator below  $T_N=140$  K. Holes introduced into the Ti(IV)/Ti(III) redox couple are not small polarons; they are spread over several ( $\approx 16$ ) Ti centers in what can be described as hole-rich clusters of itinerant electrons embedded in a hole-poor matrix of strongly correlated Ti-3d electrons. Coulomb forces keep the clusters separated. As the oxidation state increases, the volume fraction of itinerant-electron regions increases to a percolation limit near  $\delta=0.05$ . For  $\delta \geq 0.08$ , the hole-poor regions have become a minority phase within an itinerant-electron matrix, and the coupling between isolated antiferromagnetic regions becomes weaker as  $\delta$  increases until only strong-correlation superparamagnetic fluctuations are left in the itinerant-electron matrix. This behavior can be understood to be a consequence of a double-well potential for the (Ti-O) bond that is predicted from the virial theorem to occur at the crossover from strongly correlated (or localized) to itinerant electronic behavior.

## ACKNOWLEDGMENTS

The NSF and the Robert A. Welch Foundation of Houston, TX, are thanked for financial support.

- <sup>1</sup>Y. Okimoto, T. Katsufuji, Y. Okada, T. Arima, and Y. Tokura, *Phys. Rev. B* **51**, 9581 (1995).
- <sup>2</sup>J. P. Goral and J. E. Greedan, *J. Magn. Magn. Mater.* **37**, 315 (1983).
- <sup>3</sup>J. P. Goral, J. E. Greedan, and D. A. MacLean, *J. Solid State Chem.* **43**, 244 (1982).
- <sup>4</sup>G. I. Meijer, W. Henggeler, J. Brown, O.-S. Becker, J. G. Bednorz, C. Rossel, and P. Wachter, *Phys. Rev. B* **59**, 11832 (1999).
- <sup>5</sup>Y. Fujishima, Y. Tokura, T. Arima, and S. Uchida, *Phys. Rev. B* **46**, 11167 (1992).
- <sup>6</sup>K. Kumagai, T. Suzuki, Y. Taguchi, Y. Okada, Y. Fujishima, and Y. Tokura, *Phys. Rev. B* **48**, 7636 (1993).
- <sup>7</sup>Y. Tokura, Y. Taguchi, Y. Okada, Y. Fujishima, T. Arima, K. Kumagai, and Y. Iye, *Phys. Rev. Lett.* **70**, 2126 (1993).
- <sup>8</sup>C. C. Hays, J.-S. Zhou, J. T. Markert, and J. B. Goodenough, *Phys. Rev. B* **60**, 10367 (1999).
- <sup>9</sup>Y. Taguchi, T. Okuda, M. Ohashi, C. Murayama, N. Môri, Y. Iye, and Y. Tokura, *Phys. Rev. B* **59**, 7917 (1999).
- <sup>10</sup>M. J. MacEachern, H. Dabkowska, J. D. Garrett, G. Amow, W. Gong, G. Liu, and J. E. Greedan, *Chem. Mater.* **6**, 2092 (1994).
- <sup>11</sup>J. B. Goodenough, J.-S. Zhou, and J. Chan, *Phys. Rev. B* **47**, 5275 (1993).
- <sup>12</sup>J.-S. Zhou, J. B. Goodenough, and B. Dabrowski, *Phys. Rev. B* **67**, 020404(R) (2003).
- <sup>13</sup>Y. Okada, T. Arima, Y. Tokura, C. Murayama, and N. Môri, *Phys. Rev. B* **48**, 9677 (1993).
- <sup>14</sup>T. Katsufuji, Y. Taguchi, and Y. Tokura, *Phys. Rev. B* **56**, 10145 (1997).
- <sup>15</sup>J. B. Goodenough, *J. Solid State Chem.* **1**, 349 (1970)
- <sup>16</sup>J. B. Goodenough and J.-S. Zhou, *Struct. Bonding (Berlin)* **98**, 1 (2001).
- <sup>17</sup>J. B. Goodenough and J.-S. Zhou, *Struct. Bonding (Berlin)* **98**, 17 (2001).
- <sup>18</sup>A. Fujimori, I. Hase, H. Namatame, Y. Fujishima, Y. Tokura, H. Eisaki, S. Uchida, K. Takegahara, and F. M. F. de Groot, *Phys. Rev. Lett.* **69**, 1796 (1992).
- <sup>19</sup>G. I. Bersuker and J. B. Goodenough, *Physica C* **274**, 267 (1997).
- <sup>20</sup>F. Rivadulla, J.-S. Zhou, and J. B. Goodenough, *Phys. Rev. B* **67**, 165110 (2003).
- <sup>21</sup>N. F. Mott and H. Jones, *The Theory of the Properties of Metals and Alloys* (Dover, New York, 1958).
- <sup>22</sup>Z.-L. Huang, W. Bensch, D. Benea, and H. Ebert, *J. Solid State Chem.* **177**, 3245 (2004).